

## Nanoscale Chemical Imaging of Three-Way Catalyst Pt/Ce<sub>2</sub>Zr<sub>2</sub>O<sub>x</sub> Particles by Ptychographic-XAFS

Makoto Hirose<sup>1,2,\*</sup>, Nozomu Ishiguro<sup>2</sup>, Kei Shimomura<sup>1,2</sup>, Hirosuke Matsui<sup>2,3</sup>, Mizuki Tada<sup>2,3</sup>, and Yukio Takahashi<sup>1,2</sup>

<sup>1</sup>. Graduate School of Engineering, Osaka University, 2-1 Yamada-oka, Suita, Osaka 565-0871, Japan

<sup>2</sup>. RIKEN SPring-8 Center, 1-1-1 Kouto, Sayo-cho, Sayo, Hyogo 679-5198, Japan

<sup>3</sup>. Graduate School of Science, Nagoya University, Furo-cho, Chikusa, Nagoya, Aichi 464-8602, Japan

[hirose@up.prec.eng.osaka-u.ac.jp](mailto:hirose@up.prec.eng.osaka-u.ac.jp)

X-ray ptychography is a scanning version of coherent X-ray diffractive imaging for reconstructing a complex transmission function of an extended object with a spatial resolution beyond the technical limitation of the fabrication accuracy of the X-ray lens [1]. One of the most important applications of X-ray ptychography is a combination with X-ray absorption spectroscopy called ptychographic-XAFS (X-ray Absorption Fine Structure). This approach can discriminate chemical state of the specimen at the nanoscale from the reconstructed spatially resolved XAFS spectrum. So far, ptychographic-XAFS was applied to observe thin materials using soft X-rays [2,3]. To observe micrometer-sized bulk materials, it is necessary to use hard X-rays. A challenge towards realizing ptychographic-XAFS in the hard X-ray region was the accurate reconstruction of the weak XAFS signals. To overcome this problem, we proposed the advanced iterative phase retrieval algorithm using the Kramers–Kronig relation (KKR) between absorption and phase shift as an additional constraint. In a proof-of-principle experiment, XAFS spectra of a Mn<sub>2</sub>O<sub>3</sub> film around Mn-K edge (6.539 keV) was successfully reconstructed [4]. Here, ptychographic-XAFS was applied to micrometer-sized three-way catalyst materials.

Ce-based mixed oxides are known as efficient oxygen storage/release materials and used for promoter in three-way automobile exhaust cleaning systems. Especially, Ce<sub>2</sub>Zr<sub>2</sub>O<sub>x</sub> (CZ<sub>x</sub>, x=7-8) solid-solution materials attract attention due to their excellent oxygen storage property [5]. However, the heterogeneity of the CZ<sub>x</sub> prevented understanding of the real reaction behaviour by conventional methods. Ptychographic-XAFS is utilized to understand the nanoscale heterogeneity of the CZ<sub>x</sub> particles. 1 wt% Pt-supported CZ<sub>x</sub> particles (Pt/CZ<sub>x</sub>) were treated with H<sub>2</sub> or O<sub>2</sub> to produce micron-sized fully reduced Pt/CZ7, fully oxidized Pt/CZ8, and partially oxidized Pt/CZ7.6, then these particles were dispersed on 500-nm-thick Si<sub>3</sub>N<sub>4</sub> membranes. Ptychographic-XAFS experiment was carried out at BL29XUL SPring-8. Twenty-eight X-ray energies were used between 5.707–5.817 keV, including Ce-L<sub>3</sub> edge. Incident X-rays onto the samples were two-dimensionally focused to a spot size of 500 nm at full width at half maximum by a pair of Kirkpatrick–Baez (KB) mirrors. The samples were scanned in 9 by 9 positions with a step size of 400 nm. This scan condition results in the reliable image reconstruction despite of the relatively small overlap ratio since the focusing beam by KB mirrors has strong subpeaks. Multiple diffraction patterns were measured using an in-vacuum pixel-array detector (EIGER 1M) with an exposure time of 4.0 s. Intermediate valence can be decided by using the fact that XAFS of Pt/CZ7.6 can be approximately expressed by a linear combination of the XAFS of Pt/CZ7 and Pt/CZ8 [6]. The pixel size of the reconstructed images was 13 nm. While Pt/CZ7 and Pt/CZ8 particles were almost fully reduced or oxidized, Pt/CZ7.6 particles exhibited a complicated oxidation state distribution derived from the differences in the oxygen storage behaviors in the local domains as shown in Fig. 1 [7].

Pt/CZ<sub>x</sub> particles intrinsically have three-dimensional heterogeneities in structure and reactivity. The

previous results, however, are projections of the three-dimensional (3D) heterogeneity along optical axis. To truly understand the mechanism of the oxygen diffusion in Pt/CZ<sub>x</sub> particles, it is necessary to combine ptychographic-XAFS with computed tomography (CT) measurement. The experimental setup was similar to that in the previous report [7]. The sample was partly oxidized multiple Pt/CZ particles whose average size was 750 nm. In the CT measurement, the sample was rotated to 61 evenly spaced angles spanning 150°. The exposure time was selected between 0.5 s and 4.0 s. After sample images at all X-ray energies and orientations are reconstructed with a field of view of  $5 \times 5 \times 2 \text{ } \mu\text{m}^3$ , a 3D valence image was obtained by applying XAFS fitting to each  $56 \times 56 \times 56 \text{ nm}^3$  area of the energy-dependent 3D absorption images. The half-period 2D spatial resolution estimated by the phase retrieval transfer function was 44.6 nm at 0.5 s exposure, and 25.4 nm at 4.0 s exposure. The 3D spatial resolution judging from the structure reconstructed was estimated to better than 100 nm. As a result, behavior of the 3D oxygen storage was clearly visualized. Moreover, histogram analysis of the 3D valence map showed the formation of the intermediate state of Pt/CZ<sub>7.5</sub> during the oxygen storage.

In this study, ptychographic-XAFS using the iterative phasing method using the KKR constraint was applied to the three-way catalyst Pt/CZ<sub>x</sub> particles in both 2D and 3D. The reconstructed images indicated the oxidation state distributions due to their domain structures. This approach can be widely applied to investigate the heterogeneity of the various functional materials.

#### References:

- [1] J. M. Rodenburg *et al*, Phys. Rev. Lett. **98** (2007) 034801.
- [2] D. A. Shapiro *et al*, Nat. Photonics **8** (2014) 765-769.
- [3] F. Author *et al*, PNAS **113** (2016) E8219.
- [4] M. Hirose *et al*, Opt. Express **25** (2017) 8593-8603.
- [5] A. Suda *et al*, J. Ceram. Soc. Jpn. **110** (2002) 126-130.
- [6] N. Ishiguro *et al*, ChemPhysChem **14** (2014) 1563-1568.
- [7] M. Hirose *et al*, Angew. Chem. Int. Ed. **130** (2018) 1490-1495.

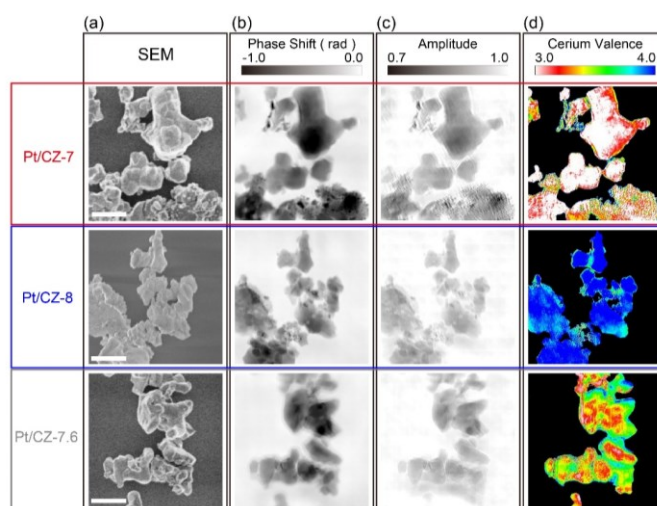


**Figure 1.** (a) SEM images of the measured samples. Reconstructed (b) amplitude, (c) phase, (d) Ce valence images of each sample. The scale bar shows 1  $\mu\text{m}$ .